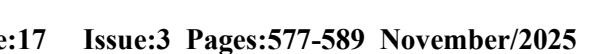


# International Journal of Engineering Research and Development

DOI: 10.29137/ijerad.1764808



Research Article

# Structure–Mechanical Property Correlation in Ba(C<sub>2</sub>H<sub>3</sub>O<sub>2</sub>)<sub>2</sub> added Bi-2212 Ceramics: Identifying Optimal Doping via Semi-Empirical Hardness Modeling

<sup>1</sup>Ali Serol Ertürk , <sup>2</sup>Mustafa Burak Türköz , <sup>3</sup>Ümit Erdem , <sup>4</sup>Gürcan Yıldırım

**Final Version**: 30/11/2025

#### Abstract

This comprehensive study investigates the effect of barium acetate (Ba( $C_2H_3O_2$ )<sub>2</sub>) impurity ion addition, in the range of 0.00–0.12 mole-to-mole ratios, on the key mechanical performance, characteristics and true mechanical microhardness ( $H_v$ ) in the plateau limit (PL) areas of bulk Bi<sub>2.1</sub>Sr<sub>2.0</sub>Ca<sub>1.1</sub>Cu<sub>2.0</sub>O<sub>7</sub>+(Ba( $C_2H_3O_2$ )<sub>2</sub>)<sub>x</sub> ceramic structures, using microhardness measurement tests under applied loads intervals 0.295 N to 2.940 N. A suite of semi-empirical mechanical modeling approaches, including elastic/plastic deformation (EPD), Meyer's Law (ML), modified proportional sample resistance (MPSR), proportional sample resistance (PSR), and Hays–Kendall (HK) mechanical approaches is employed to evaluate changes in mechanical performance within the PL regions. The results show that the incorporation of Ba( $C_2H_3O_2$ )<sub>2</sub> impurity ion addition progressively degrades intrinsic slip systems and mechanical durability. As a result, undoped Bi-2212 ceramic structure exhibits the lowest sensitivity to external loads, while the most heavily doped composition displays the highest susceptibility to applied loads. All Bi<sub>2.1</sub>Sr<sub>2.0</sub>Ca<sub>1.1</sub>Cu<sub>2.0</sub>O<sub>7</sub>+(Ba( $C_2H_3O_2$ )<sub>2</sub>)<sub>x</sub> ceramic structures ceramics exhibit the characteristic indentation size effect (ISE) performance. Among the mechanical investigation models examined, the HK approach yields hardness values in the plateau regions that most closely match the experimentally measured  $H_v$  parameters, confirming its superiority and reliability for the mechanical characterization of Bi-2212 systems containing barium acetate impurity ions.

## Kevwords

Bi-2212 phase, Ba(C<sub>2</sub>H<sub>3</sub>O<sub>2</sub>)<sub>2</sub> addition, Hv, True Hv values, HK mechanical approach.

 $<sup>^{1}</sup> A diyaman\ University\ Department\ of\ Basic\ Pharmaceutical\ Sciences,\ 02030,\ Adiyaman, TURKIYE$ 

<sup>&</sup>lt;sup>2</sup>Karabuk University Department of Electric Electronic Engineering, 78010, Karabük, TÜRKİYE <sup>3</sup>Kırıkkale University Department of Electronics and Automation, 71400, Kırıkkale, TÜRKİYE

<sup>&</sup>lt;sup>4</sup>Abant Izzet Baysal University, Department of Mechanical Engineering, 14100, Bolu, TÜRKİYE

<sup>\*</sup> Corresponding Author: umiterdem@kku.edu.tr

#### 1. Introduction

The accelerating pace of technological and industrial development has sharply increased global demands for efficient energy production, transmission, and utilization. Meeting these requirements in fields such as heavy industry, energy engineering, metallurgy, and advanced manufacturing depends not only on optimizing energy management but also on selecting materials with exceptional mechanical durability. Over recent decades, engineering efforts have focused on designing new materials or enhancing existing ones to achieve superior stiffness, strength, hardness, ductility, toughness, and overall service life. Such improvements contribute to sustainable development by enabling resource conservation, climate protection, and cost reduction (Turkoz et al., 2020). Hardness is a fundamental mechanical property that reflects a material's resistance to permanent deformation and acts as a practical indicator of wear resistance, load-carrying capacity, and mechanical durability to applied loads (Askeland et al., 2020; Smith et al., 2020). In hardness testing, a controlled force is applied to a specimen using a precisely shaped indenter, and the depth or size of the resulting impression is measured. Softer materials produce deeper and larger indentations, yielding lower hardness values, whereas harder materials generate smaller impressions and higher hardness values (Chattopadhyay et al., 2020).

Compared to other mechanical tests, hardness measurements offer notable advantages, including minimal sample preparation, low equipment cost, rapid testing, high accuracy, and the potential to evaluate additional mechanical parameters from the same dataset (Müler et al., 2019; Tancret et al., 2020). Standard testing techniques include Rockwell, Brinell, and microindentation methods. Especially, the latter (Vickers and Knoop tests) methods are particularly suitable for brittle materials such as mica-like structures and high-temperature superconducting ceramics. Microindentation employs small loads (typically between 1 g and 1000 g) and a diamond indenter to assess localized regions of a specimen, enabling precise measurement of hardness gradients and defect-sensitive areas (Callister et al.). Modern Vickers microhardness testing, supported by automated data acquisition systems, provides highly reproducible results and allows indirect determination of other mechanical quantitates; namely, yield strength, elastic modulus, brittleness index, mechanical strength, fracture toughness, and elastic stiffness. This versatility makes microindentation an essential tool for evaluating advanced ceramics, where both mechanical integrity and functional performance are critical to real-world applications.

In this work, we examine the influence of partially incorporating barium acetate (Ba(C2H3O2)2) into Bi-2212 high-temperature superconductors, with the objective of enhancing phase stability, mechanical strength, and overall durability. The investigation is carried out using Vickers microhardness tests under varying applied loads (Kara et al., 2020; Erdem et al., 2020). The selection of barium acetate is motivated by its high intrinsic hardness and paramagnetic nature, which are anticipated to strengthen interatomic bonding, activate slip systems, and improve resistance to externally applied forces. Bi-2212 ceramics are well recognized for their thermodynamic stability, high critical temperature, and capacity to sustain large current densities even under intense magnetic fields, making them indispensable in energy, transportation, and medical technologies (Hannachi et al., 2020; Fallah-Arani et al., 2017; Slimani et al., 2015; Zagura et al., 2018; Jeong et al., 2013). Furthermore, their layered crystal structure facilitates the fabrication of long-length wires and tapes, while maintaining structural integrity under high-temperature and humid environments (Xu et al., 2020; Harabor et al., 20; Abdelhaleem et al., 20; Hassan et al., 2019; Sheahen et al., 20; Takayama-Muromachi et al., 1999; Plakida et al., 2020). The Bi-2212 phase is an ideal candidate for advanced engineering applications owing to these attributes such as low energy dissipation, high current-carrying capability, and strong magnetic field tolerance. In this study, partial substitution with barium acetate is employed to further improve its critical mechanical characteristics, and the resultant materials are systematically evaluated through Vickers microhardness measurements to establish the relationship between barium content and mechanical performance.

Mechanical properties are assessed using Vickers microhardness testing methods under loads of 0.245–2.940 N, a technique well-suited for brittle, heterogeneous superconductors. Data are inspected using five mechanical characterization models, including, elastic/plastic deformation (EPD), Hays–Kendall (HK), Meyer's Law (ML), proportional sample resistance (PSR), and modified PSR (MPSR) with a focus on plateau limit regions, where load-independent Hv values are most meaningful. Among them, the MPSR model proved most accurate for determining true Hv values. Results show that the existence and enhancement of (Ba(C2H3O2)2) impurity ion content degrades the optimization of mechanical durability, crystal quality, mechanical strength, elastic recovery, tetragonal phase stability, and resistance to deformation (Zhao et al., 2024; Chang et al., 2025). This integrated experimental–modeling approach establishes a clear link between microstructural evolution and mechanical behavior, providing guidance for the design of high-performance Bi-2212-based superconducting ceramics.

# Symbols and Abbreviations

EPD Elastic/Plastic Deformation

HK Hays-Kendall ML Meyer's Law

PSR Proportional Sample Resistance

MPSR Modified Proportional Sample Resistance

Hv Hardness Vicker F Applied Load

ISE Indentation Size Effect
RISE Reverse Identation Size Effect

α Indenter Face Angle

A<sub>Meyer</sub> Hardness-related Constant

x Doping Ratio

w Characteristic constant

d Notch Depth

HHK
 d<sub>p</sub>
 de
 Diagnostic Coefficient
 β
 Microhardness Coefficient

WMPSR Minimum Indentation Load Parameter

## 2. Materials and Methods

This work builds upon the systematic characterization of Ba(C<sub>2</sub>H<sub>3</sub>O<sub>2</sub>)<sub>2</sub> impurity ions added Bi<sub>2.1</sub>Sr<sub>2.0</sub>Ca<sub>2.1</sub>Cu<sub>3.0</sub>O<sub>y</sub> ceramic materials reported in (Ulgen et al., 20; Ulgen et al., 20). The present work methodically addresses preparation process of bulk Bi<sub>2.1</sub>Sr<sub>2.0</sub>Ca<sub>1.1</sub>Cu<sub>2.0</sub>O<sub>2</sub>+(Ba(C<sub>2</sub>H<sub>3</sub>O<sub>2</sub>)<sub>2</sub>)x ceramic structures, covering critical aspects, including precursor powder purity, solid-state reaction processes, calcination, and sintering conditions. The preparation route is supported by detailed considerations of heat-treatment parameters, including calcination-sintering temperatures, heating-cooling ratios, press loads and durations, and milling procedures, as well as the minimization of powder impurities. Bulk samples were synthesized with additional barium acetate impurity ion contents of x= 0.00, 0.03, 0.05, 0.07, 0.09, and 0.13, hereafter referred to as pure, BiBaC-1, BiBaC-2, BiBaC-3, BiBaC-4, and BiBaC-5 respectively. References (Ulgen et al., 20) and (Ulgen et al., 20) provide an in-depth description of these preparation procedures and also reports complementary results on the electrical conductivity, resistivity, and superconducting characteristics of samples. Mechanical behavior is examined using Hv measurement tests performed in air using a SHIMADZU HVM-2 digital microhardness tester under applied loads of 0.245, 0.490, 0.980, 1.960, and 2.940 N. Diamond indenter within pyramidal shape is applied to the specimen surfaces for 10 seconds per test, and each measurement is repeated five times to ensure accuracy. The average diagonal sizes of the indentations determined with a microscope are used to calculate Hv values. The experimental design enables the assessment of the effects of Ba(C2H3O2)2 impurity ion content on critical mechanical and microstructural characteristics in the plateau limit (PL) regions, including critical crack length, stored internal strain energy, and crystal structure integrity. To extract true Hv values and evaluate load-independent mechanical properties, the experimental data are inspected by means of five mechanical approaches: the PSR, MPSR, HK, EPD, and ML approaches. All samples exhibit the standard indentation size effect (ISE) behavior. Comparative analysis revealed that the MRPS, EPD, and particularly the HK models provide the closest agreement with experimental Hv parameters in the PL regions. Accordingly, while results from all models are reported, the discussion primarily emphasizes the mechanical insights derived from these three superior modeling approaches, with the HK model demonstrating the highest accuracy for evaluating true HV parameters in the Bi-2212 ceramics containing barium acetate Ba(C2H3O2)2 impurity ion addition.

## 3. Result and Discussion

In the current work, Hv measurements are used to establish correlations between barium acetate  $(Ba(C_2H_3O_2)_2)$  addition impurity ion concentration and the formation of stress regions, intergranular interactions, artificial force barriers, and slip systems. These correlations provide valuable information about the observed variations in mechanical durability, strength, and other characteristic properties arising from  $Ba(C_2H_3O_2)_2$  impurity ions added bulk Bi-2212 ceramic lattice. The Hv hardness values are calculated from the applied loads (F) and corresponding average diagonal lengths (d) using:

$$Hv = 1854.4 \left(\frac{F}{d^2}\right) \text{(GPa)}$$
 (1)

here F is in the unit of Newtons, d in millimeters, and constant 1.8544 is derived from the indenter face angle ( $\alpha = 136^{\circ}$ ). The Hv-load curves for the pure, BiBaC-1, and BiBaC-1 ceramics are presented in Fig. 1 and BiBaC-3, BiBaC-4, and BiBaC-5 ceramic structures Fig. 2, respectively. This study is entirely based on semi-empirical mechanical modelling for Ba(C<sub>2</sub>H<sub>3</sub>O<sub>2</sub>)<sub>2</sub> impurity ions added Bi-2212 crystal systems. Firstly, we will give the main discussions related to the variation of fundamental mechanical performance results of Bi-2212 crystal lattices with the Ba(C<sub>2</sub>H<sub>3</sub>O<sub>2</sub>)<sub>2</sub> impurity addition. It is obvious from the figures that Ba(C<sub>2</sub>H<sub>3</sub>O<sub>2</sub>)<sub>2</sub> impurity ion addition mechanism negatively affects the durability, mechanical strength, and fundamental characteristics of Bi-2212 ceramics structures. This degradation is attributed to reduction of key performance indicators, including the formation of artificial force barriers, weakening of host–dopant chemical bonds, decreased crystal quality, weak intergranular interactions, localized stress redistribution, diminished interlayer connections, and activation of additional slip systems.

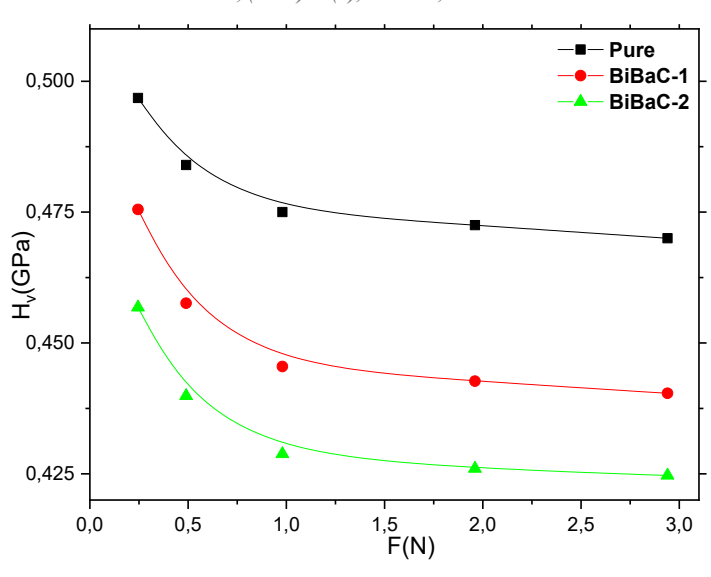


Figure 1. Variation of microhardness values with applied loads for pure, BiBaC-1, and BiBaC-2 ceramic structures

The results indicate that  $Ba(C_2H_3O_2)_2$  impurity contributions are successfully incorporated into Bi-2212 ceramic systems as intended. On this basis, it is found that mechanical durability degrades with addition mechanism and for the maximum addition level of x=0.13 Hv reaches lowest values. At this level, the elastic recovery is damaged remarkably, declining the tetragonal phase and accelerating dislocation and crack propagation even under external test loads (Callister et al.) due to the increased reversible-to-irreversible deformation ratio. Also, excess  $Ba(C_2H_3O_2)_2$  impurity ions cause a sharp increase in microscopic crystallinity defects, accelerating stress-induced phase transformations and leading to mechanical deterioration (Dogruer et al., 20). Consequently, fracture and breakage occur under lower applied loads. The numerical values obtained from the Figs. 1 and 2 are given in Table 1 to showcase the change of the mechanical characteristics of Bi-2212 ceramic structures based on the addition mechanism.

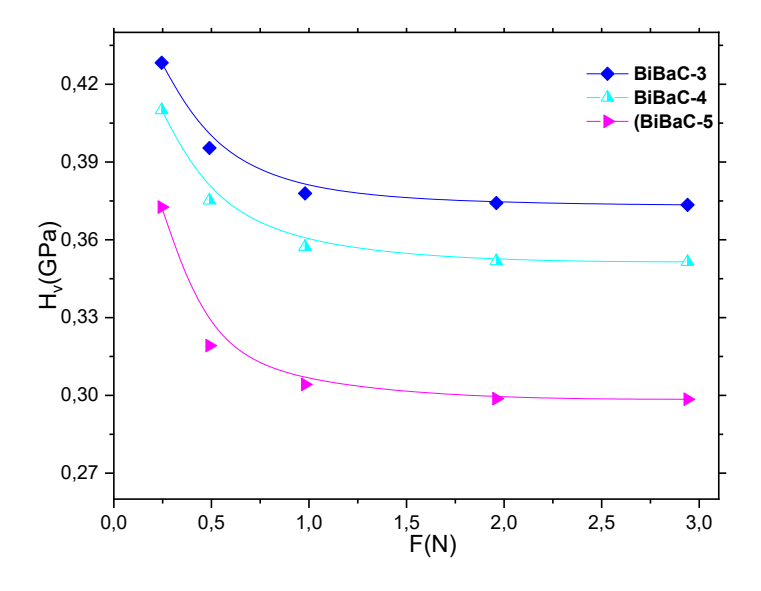


Figure 2. Change of microhardness values with loads belonging to BiBaC-3, BiBaC-4, and BiBaC-5 materials

**Table 1.** Mechanical microhardness parameters for pure and  $Bi_{2.1}Sr_{2.0}Ca_{1.1}Cu_{2.0}O_{\gamma} + (Ba(C_2H_3O_2)_2)_x$  ceramics under different applied

| Samples | F (N) | Hv (GPa) |  |  |
|---------|-------|----------|--|--|
|         | 0.249 | 0.4968   |  |  |
|         | 0.490 | 0.4840   |  |  |
| Pure    | 0.980 | 0.4750   |  |  |
|         | 1.960 | 0.4725   |  |  |
|         | 2.940 | 0.4700   |  |  |
|         | 0.249 | 0.4755   |  |  |
|         | 0.490 | 0.4576   |  |  |
| BiBaC-1 | 0.980 | 0.4455   |  |  |
|         | 1.960 | 0.4427   |  |  |
|         | 2.940 | 0.4404   |  |  |
|         | 0.249 | 0.4568   |  |  |
|         | 0.490 | 0.4399   |  |  |
| BiBaC-2 | 0.980 | 0.4288   |  |  |
|         | 1.960 | 0.4260   |  |  |
|         | 2.940 | 0.4247   |  |  |
|         | 0.249 | 0.4283   |  |  |
|         | 0.490 | 0.3954   |  |  |
| BiBaC-3 | 0.980 | 0.3779   |  |  |
|         | 1.960 | 0.3742   |  |  |
|         | 2.940 | 0.3735   |  |  |
|         | 0.249 | 0.4100   |  |  |
|         | 0.490 | 0.3752   |  |  |
| BiBaC-4 | 0.980 | 0.3573   |  |  |
|         | 1.960 | 0.3518   |  |  |
|         | 2.940 | 0.3515   |  |  |
|         | 0.249 | 0.3726   |  |  |
|         | 0.490 | 0.3192   |  |  |
| BiBaC-5 | 0.980 | 0.3042   |  |  |
|         | 1.960 | 0.2987   |  |  |
|         | 2.940 | 0.2985   |  |  |

Table 1 indicates that the pure Bi-2212 compound has the highest hardness values between approximately 0.4968 and 0.4700 GPa under test loads intervals of 0.245 N-2.940 N, respectively. The decreasing trend depending on the loads reflects the typical indentation size effect (ISE) behavior of Bi-2212 crystal systems. Increasing Ba(C2H3O2)2 ion incorporation reduces both the Hv values and the ISE tendency at all applied loads. As for the Hv values for the bulk BiBaC-5 compound, the Hv smallest parameters of 0.3726, 0.3192, 0.3042, 0.2987, and 0.2985 GPa are obtained at 0.245 N, 0.490 N, 0.980 N, 1.960 N, and 2.940 N, respectively. The obtained hardness values are used to examine the load-independent Hv values in PL zones. We also highlight the applicability and effectiveness of semiempirical modeling approaches in evaluating the mechanical behavior of Bi-2212 advanced ceramic systems, thereby providing insight into their potential for real-world applications, long-term performance, and service-life optimization. Accordingly, the loadindependent Hv data within PL zones are inspected with the use of five established theoretical models: PSR, HK, EPD, ML, and MPSR approaches (Elmustafa et al., 20; Saxena et al., 20; Khalil et al., 20). By systematically comparing the mentioned Hv results obtained from the mentioned models, the most appropriate approaching framework is identified for Ba(C2H3O2)2 impurity ion content added Bi-2212 ceramics, enabling a detailed evaluation of their mechanical durability, strength, and deformation behavior. This comparative assessment allows for a comprehensive understanding of how different mechanical models interpret load-independent microhardness and predict the mechanical performance of the studied ceramics. The first model applied is Meyers' Law (ML), which is used to investigate the role of Ba(C2H3O2)2 impurity ion content concentration on essential mechanical parameters, including strength, critical stress values, elastic recovery, crack and deformation constraints, deformation degree, tetragonal phase stability, and load sensitivity.

# 3.1. Mechanical characteristics analysis via meyers' law mechanical model

Meyers' Law is employed to evaluate load-independent Hv zones, and to distinguish between indentation size effect (ISE) and reverse ISE (RISE) behaviors (Zalaoglu et al., 20). In this model (given in Fig. 3), the mechanical response is characterized by the Meyer coefficient (n), derived from the relationship between the applied indentation load (F) and the average indentation diagonal (d) according to (Mohammed et al., 20):

$$F = A_{MEYER} d^n (2)$$

Here,  $A_{Meyer}$  represents the hardness-related constant, while n points out a key diagnostic parameter: n > 2 indicates RISE behavior, n < 2 corresponds to typical ISE behavior, and n = 2 signifies complete load-independence of hardness (Ling et al., 19).

In this study, n values for bulk  $Bi_{2.1}Sr_{2.0}Ca_{1.1}Cu_{2.0}O_{\gamma}$  +(  $Ba(C_2H_3O_2)_2$ )x cuprates are extracted from LnF versus Lnd plots, with results summarized in Table 2. All samples exhibit n < 2, confirming standard ISE behavior, where both elastic and plastic deformations occur simultaneously within the crystal lattice. The n values vary notably with  $Ba(C_2H_3O_2)_2$  impurity ion addition level, reflecting the influence of  $Ba(C_2H_3O_2)_2$  impurity incorporation on the mechanical response.

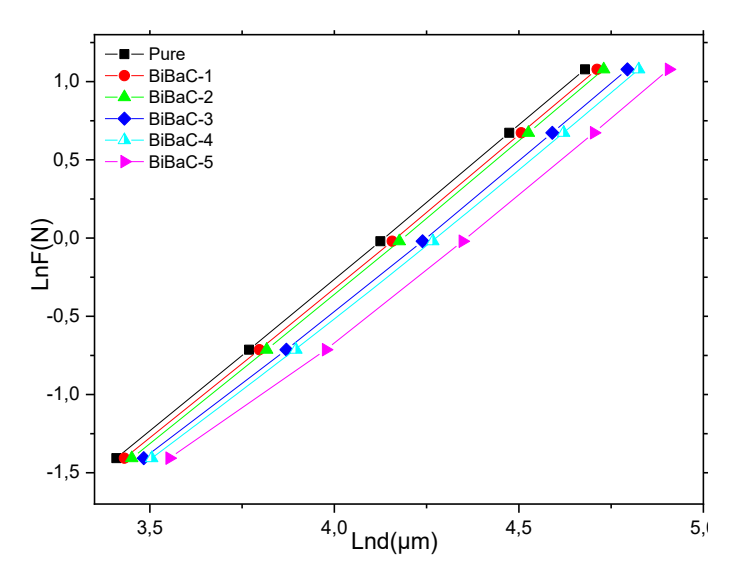


**Figure 3.** Relations between the natural logarithm of the applied test force, Ln(F), and natural logarithm of indentation size, Ln(d), for Hv measurements under different loads in pure Bi-2212 and Ba(C<sub>2</sub>H<sub>3</sub>O<sub>2</sub>)<sub>2</sub> impurity added Bi-2212 ceramic structures.

Up to x = 0.08, n values remain above 1.9, indicating relatively low load sensitivity. However, beyond x = 0.08, a pronounced decrease below 1.9 is observed, coinciding with a marked increase in deformation degree and stored internal strain energy, which promote crack propagation. This trend correlates well with the steep decline in Hv values already evident in Fig. 3.

**Table 2.** HK, MPSR, PSR, EPD, and ML mechanical approach constants for pure Bi-2212 and Ba(C<sub>2</sub>H<sub>3</sub>O<sub>2</sub>)<sub>2</sub> impurity added ceramic structures

|         | Meyer's<br>Law  |   | PSR Model                    |  | MPSR Model                         |   |  | EPD Model                                |                                      | HK Model                  |                                   |
|---------|---|---|------------------------------|--|------------------------------------|---|--|--|--------------------------------------|---------------------------|-----------------------------------|
| Samples | $\begin{array}{c} A_{MEYER} \\ x10^{-4} \\ (N/\mu m^2) \end{array}$ | n | αx10 <sup>-4</sup><br>(N/μm) | $\beta x 10^{-4}$ (N/ $\mu$ m <sup>2</sup> ) | Wx10 <sup>-</sup> <sup>2</sup> (N) | $\begin{array}{c} A_{0MPSR} \\ x10^{-3} \\ (N/\mu m) \end{array}$ | $\begin{array}{c} A_{1PSR} \\ x10^{-4} \\ (N/\mu m^2) \end{array}$ | d <sub>e</sub> x10 <sup>-1</sup><br>(μm) | $A_{2EPD}x10^{-1}$ $(N^{1/2}/\mu m)$ | Wx10 <sup>-1</sup><br>(N) | Азнк х10 <sup>-4</sup><br>(N/μm²) |
| Pure    | 3.074   | 1 | 5.611                        | 2.481  | 0.722                              | 0.285   | 2.503  | 0.174                                    | 0.158                                | 0.156                     | 2.523                             |
| BiBaC-1 | 3.099   | 1 | 7.289                        | 2.306  | 1.860                              | 0.046   | 2.357  | 0.233                                    | 0.152                                | 0.200                     | 2.360                             |
| BiBaC-2 | 2.955   | 1 | 2.226                        | 6.740  | 2.373                              | -0.176  | 2.288  | 0.219                                    | 0.149                                | 0.183                     | 2.276                             |
| BiBaC-3 | 3.215   | 1 | 11.135                       | 1.910  | 5.714                              | -0.841  | 2.044  | 0.382                                    | 0.138                                | 0.298                     | 1.991                             |
| BiBaC-4 | 3.219   | 1 | 12.314                       | 1.784  | 6.180                              | -0.824  | 1.921  | 0.434                                    | 0.134                                | 0.342                     | 1.870                             |
| BiBaC-5 | 3.334   | 1 | 14.845                       | 1.484  | 8.747                              | -1.270  | 1.656  | 0.558                                    | 0.122                                | 0.418                     | 1.583                             |

To validate the suitability and predictive accuracy of the selected mechanical models, regression analysis was performed using the adjusted coefficient of determination as the primary statistical metric. The values are calculated for each sample across all models to assess the strength of correlation between the experimental results and model predictions (Table 3). The adjusted coefficient of determination values for the present pure and  $Bi_{2.1}Sr_{2.0}Ca_{1.1}Cu_{2.0}O_{\gamma}$  +(  $Ba(C_2H_3O_2)_2$ )x ceramics for all investigated models, including Meyer's Law, PSR, MPSR, EPD, and HK are found to be consistently above 0.997, confirming an excellent agreement between the experimental Vickers microhardness data and theoretical predictions across both undoped and Ba-doped Bi-2212 ceramics. For the pure sample, all models yield nearly identical fits (>0.9999), indicating uniform applicability in the absence of doping. In  $Ba(C_2H_3O_2)_2$ 

impurity ion doped samples, the MPSR and HK approaches demonstrate perfect fits (= 1) in several cases, displaying superior capability in capturing the load–hardness relationship under modified microstructural conditions.

| Table 3   | Dagracion  | volues fo | r cuitability | and | predictive a | couroca | oftha   | alactad  | machanical | modals |
|-----------|------------|-----------|---------------|-----|--------------|---------|---------|----------|------------|--------|
| i abie 3. | Regression | values 10 | Sultability   | anu | predictive a | ccuracy | or me s | serected | mechanicai | models |

| Samples | (Adj) R <sup>2</sup> |         |         |         |         |  |  |  |
|---------|----------------------|---------|---------|---------|---------|--|--|--|
|         | MEYER' LAW           | PSR     | MPSR    | EPD     | HK      |  |  |  |
| Pure    | 0.99995              | 0.99997 | 0.99999 | 0.99999 | 0.99999 |  |  |  |
| BiBaC-1 | 0.99988              | 0.99989 | 1       | 0.99998 | 1       |  |  |  |
| BiBaC-2 | 0.99987              | 0.99987 | 0.99999 | 0.99997 | 1       |  |  |  |
| BiBaC-3 | 0.99939              | 0.99921 | 0.99999 | 0.99983 | 0.99997 |  |  |  |
| BiBaC-4 | 0.99931              | 0.99913 | 1       | 0.99982 | 0.99997 |  |  |  |
| BiBaC-5 | 0.99795              | 0.99730 | 0.99999 | 0.99948 | 0.99993 |  |  |  |

A marginal reduction in fit quality is observed at the highest  $Ba(C_2H_3O_2)_2$  content (BiBaC-5), particularly for the PSR and Meyer's Law models, which may be attributed to increased microstructural heterogeneity and defect density at elevated doping levels. To sum up, the consistently high—values validate the robustness of all five semi-empirical approaches, with MPSR and HK emerging as the most reliable for  $Ba(C_2H_3O_2)_2$  impurity ions added Bi-2212 systems. Among the tested compositions, the bulk BiBaC-5 material displays the lowest mechanical performance, attributable to diminished critical performance indicators, reduced elastic recovery capacity, and a destabilized tetragonal phase. These changes are linked to increased microstructural defects and crystallinity degradation at higher  $Ba(C_2H_3O_2)_2$  impurity ion incorporation contents. Numerically, the highest n value is determined to be about 1.958 for the pure sample, whereas the lowest n value of 1.845 belongs to the BiBaC-5 ceramic material. The  $A_{Meyer}$  constants provided in Table 2 are found to be positive for all compositions, consistent with the presence of ISE behavior ascribing to the  $Ba(C_2H_3O_2)_2$  impurity added Bi-2212 ceramic structures (Hays et al., 19). Numerically, the  $A_{Meyer}$  constants are calculated to be in a range of about 2.995 x 10-4 N/ $\mu$ m2- 10-4 N/ $\mu$ m2. In summary, the ML model effectively captures the mechanical characteristic behavior of 10-4 N/10-4 # 3.2. Assessment of general mechanical performance using HK mechanical model

The Hays-Kendall mechanical model is widely recognized for its capability to evaluate critical mechanical performance indicators, including elasticity, recovery mechanism, tetragonal phase stability, structural integrity, resistance to applied loads, susceptibility to stress amplification, and deformation behavior of ceramics (especially BSCCO and YBCO superconductors) within the PL region. In this framework, a characteristic constant (W) is introduced to quantify the correlation between applied load and irreversible deformation. The governing relation is (Tarkanian et al., 19; Erdem et al., 20):

$$F - W = AHKd^2 \tag{3}$$

where AHK is determined from the extrapolation of F1/2 versus notch depth (d), as depicted in Fig. 4.

The derived parameters (Table 2) confirm that all  $Ba(C_2H_3O_2)_2$  impurity added Bi-2212 ceramic structures possess positive W constants, indicating typical ISE behavior consistent with experimental data and other model outputs. The crystal lattice demonstrates both reversible and irreversible deformation, with a notable degree of elastic recovery upon unloading. Numerically, the pure sample has the minimum W value of  $0.156 \times 10^{-1} \, \text{N}$ , whereas the maximum W value of  $0.418 \times 10^{-1} \, \text{N}$  ascribes to the BiBaC-5 ceramic material, reflecting the accumulation of irreversible crystallographic defects, increased deformation degree, and elevated internal strain energy for crack growth with impurity. As for the variation of AHK parameters with dopants, as shown in the table, the AHK values exhibit a consistent decreasing trend. On this basis, the maximum AHK value of  $2.523 \times 10^{-4} \, \text{N/µm2}$  is observed for the pure sample whereas the minimum value of  $1.583 \times 10^{-4} \, \text{N/µm2}$  is attributed to the BiBaC-5 ceramic material. This means that the inner sample exhibits the least sensitive to the applied loads, while the BiBaC-5 ceramic cuprate presents the highest response to the loads. This is because, the HK model shows that the presence and increase in the Ba( $C_2H_3O_2$ )2 impurity ion addition levels in the Bi-2212 crystal system damage seriously the mechanical integrity of Bi-2212 ceramic structures. The HK approach also enables the calculation of load-independent hardness (HHK) in PL regions via Eq. 4, with results presented in Table 4.

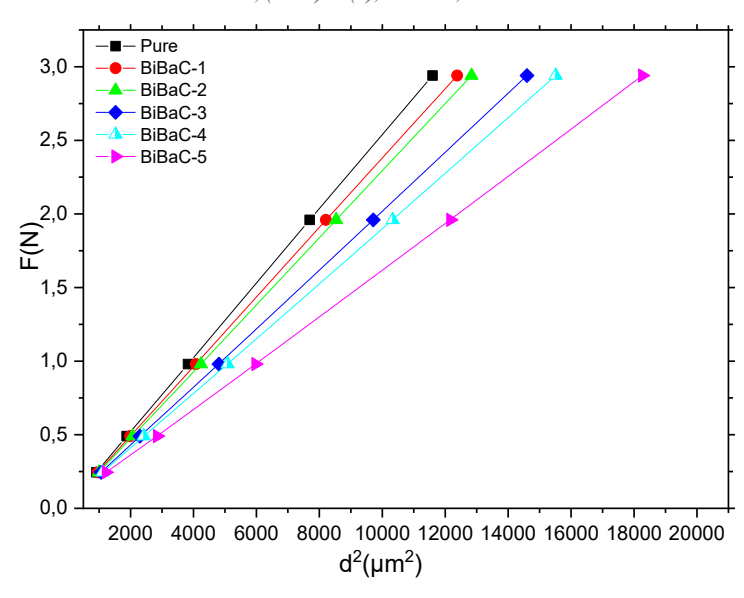


Figure 4. Differentiation of the applied test load, F (N), with respect to the squared indentation size, d² (μm²), under various loads for pure Bi-2212 and bulk Ba(C<sub>2</sub>H<sub>3</sub>O<sub>2</sub>)<sub>2</sub> impurity added Bi-2212 ceramic structures.

$$H_{HK} = 1854.4 A_{HK} \tag{4}$$

As evidenced by the data in Table 4, the Hv parameters obtained in the PL regions exhibit excellent agreement with the experimentally measured Hv values across all applied load ranges compared to other models. Accordingly, the HK model demonstrates high reliability in determining both the primary mechanical properties and the actual hardness values within the PL regions. In fact, this consistency confirms that, among all the semi-empirical models employed in this study, the HK approach provides the most reliable evaluation of mechanical performance, tetragonal phase stability, intrinsic mechanical characteristics, and load-independent Hv values in the PL regions of Ba(C<sub>2</sub>H<sub>3</sub>O<sub>2</sub>)<sub>2</sub> impurity added Bi-2212 ceramic structures. Further, the examination indicates that the predictions for all the samples studied by HK mechanical approach are found to be as the highest correlations. Thus, the model shows the highest accuracy, indicating the best model to investigate the mechanical characteristics of Ba(C<sub>2</sub>H<sub>3</sub>O<sub>2</sub>)<sub>2</sub> impurity added Bi-2212 ceramic structures.

**Table 4.** Comparison of Vickers microhardness (Hv) values obtained from PL measurements with those calculated using the MPSR, EPD, HK, and PSR mechanical models

| Samples | H <sub>PSR</sub> (GPa) | H <sub>MPSR</sub> (GPa) | Hepd (GPa) | Ннк (GPa) | Hv (GPa)    |
|---------|------------------------|-------------------------|------------|-----------|-------------|
| Pure    | 0.460                  | 0.464                   | 0.461      | 0.468     | 0.470-0.497 |
| BiBaC-1 | 0.428                  | 0.437                   | 0.428      | 0.438     | 0.440-0.475 |
| BiBaC-2 | 1.250                  | 0.424                   | 0.413      | 0.422     | 0.425-0.457 |
| BiBaC-3 | 0.354                  | 0.379                   | 0.355      | 0.369     | 0.374-0.428 |
| BiBaC-4 | 0.331                  | 0.356                   | 0.331      | 0.347     | 0.352-0.410 |
| BiBaC-5 | 0.275                  | 0.307                   | 0.277      | 0.294     | 0.298-0.373 |

## 3.3. Evaluation of fundamental mechanical characteristics via the EPD model

The Elastic—Plastic Deformation mechanical model is employed to evaluate the intrinsic mechanical performance, durability, structural integrity, load sensitivity, microhardness response, and intrinsic load-independent Hv values of Ba(C<sub>2</sub>H<sub>3</sub>O<sub>2</sub>)<sub>2</sub> impurity added Bi-2212 ceramic structures in the PL regions. This model establishes a direct relationship between the recovery mechanism and indentation depth, introducing a characteristic parameter directly related to the irreversible deformation constant (d<sub>p</sub>) to quantify permanent plastic deformation during indentation. The EPD framework is particularly effective in distinguishing between temporary elastic shape recovery and permanent plastic damage in ceramic systems under mechanical stress. The semi-empirical formulation is given by (Erden et al., 20):

$$F = A_{EPD} \left( d_{e+} d_p \right)^2 \tag{5}$$

Here, AEPD and associated constants are obtained from the extrapolation of plots of external loads (F1/2) and the average depths (dp), as shown in Fig. 5. The second parameter, de is a diagnostic coefficient for mechanical behavior classification: positive de values confirm ISE behavior, whereas negative values indicate reverse ISE nature of material.

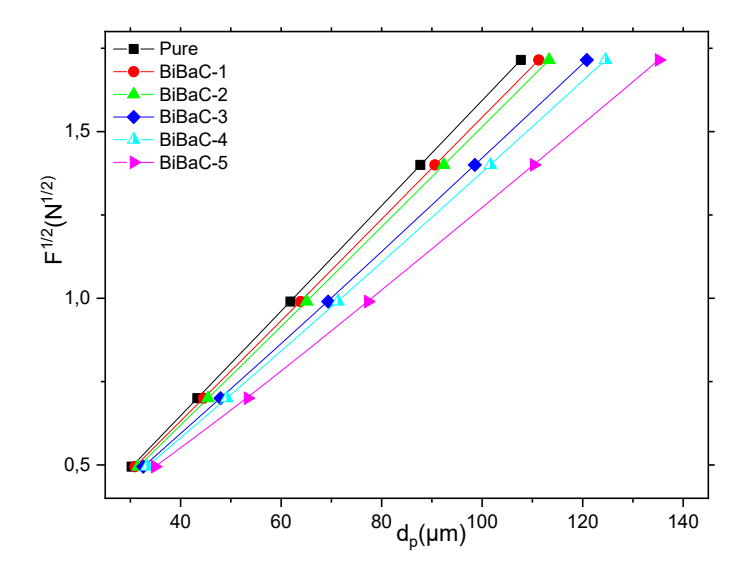


**Figure 5.** Change of the applied test load, (F1/2) in terms of the average depths (dp) under various loads for pure Bi-2212 and bulk Ba(C<sub>2</sub>H<sub>3</sub>O<sub>2</sub>)<sub>2</sub> impurity added Bi-2212 ceramic structures

As shown in Table 2, all of Ba(C<sub>2</sub>H<sub>3</sub>O<sub>2</sub>)<sub>2</sub> impurity added Bi-2212 ceramic structures possess positive de values, affirming the prevalence of ISE behavior. This observation aligns with experimental findings from other models, indicating that all compositions exhibit both elastic and plastic deformation, with elastic recovery dominating upon load removal. The impurity addition trend reveals that the AEPD parameters are noted to decrease seriously based on the addition mechanism. On this basis, the maximum AEPD value of 0.158 x 10<sup>-1</sup> N1/2/μm belongs to the pure Bi-2212 sample, whereas the AEPD value reduces regularly from 0.152 x 10<sup>-1</sup> N1/2/μm to 0.122 x 10<sup>-1</sup> N1/2/μm (for the BiBaC-5 ceramic material), respectively. Decrement trend stems from the degradation of resistance to deformation, attributed to enhanced deformation degree and higher stored internal strain energy, which facilitate crack propagation. These results show that while the unadded Bi-2212 ceramic structure is the least sensitive to external loads, BiBaC-5 ceramic material exhibits rapid crack initiation and propagation. Load-independent hardness values (H<sub>EPD</sub>) for the PL regions, calculated via Eq. 6, are provided in Table 4.

$$H_{EPD} = 1854.4A_{EPD}$$
 (6)

According to the computations provided in Table 4, the model remains inadequate for investigating load-independent Hv values in the PL regions. While not fully precise in quantifying absolute load-independent hardness, the EPD model excels in evaluating general mechanical performance, phase stability, and structural resilience, making it one of the most reliable semi-empirical approaches for assessing Ba(C2H3O2)2 impurity added Bi-2212 ceramic structures. All in all, although the EPD model successfully captures trends in mechanical performance, tetragonal phase durability, and crack propagation, it tends to underestimate actual load-independent Hv values in the PL region compared to experimental measurements.

## 3.4. Mechanical performances and characteristics based on PSR model

The Proportional Specimen Resistance mechanical model is widely recognized for its effectiveness in evaluating both load-dependent and load-independent Hv parameters of ceramic compounds. The model provides a comprehensive framework for assessing how surface energy distribution and microstructural integrity influence mechanical responses, particularly in the presence of microscopic crystallinity imperfections (Zalaoglu et al., 20). In this model, the surface energy coefficient ( $\alpha$ ) reflects the general mechanical characteristics of the material, while the microhardness coefficient ( $\alpha$ ) is directly related to resistance against deformation (Michels et al., 19; Fröhlich et al., 19). The combined analysis of  $\alpha$  and  $\beta$  allows a straightforward distinction between ISE and reverse ISE behaviors. The parameters of the PSR model are determined from Eq. 7:

$$F = \alpha d + \beta d^2 \tag{7}$$

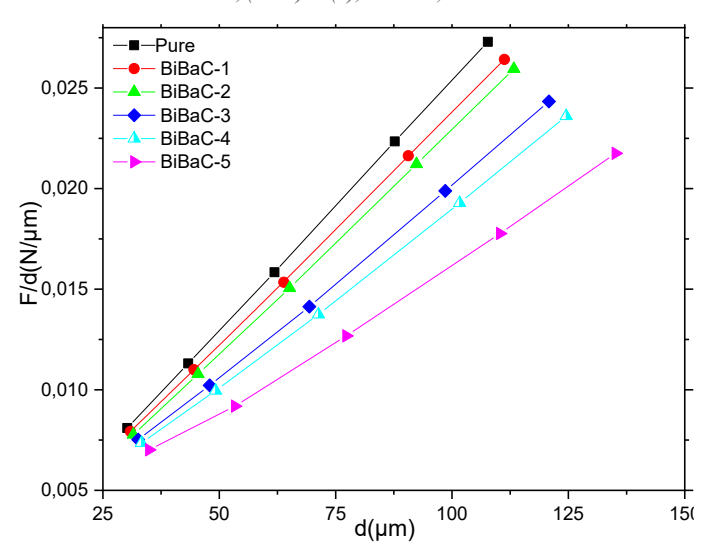


**Figure 6.** Change of the applied test load, F/d over diagonal lengths (d) under various loads for pure Bi-2212 and bulk Ba(C2H3O2)2 impurity added Bi-2212 ceramic structures

Figure 6 presents the relationships between applied test loads (F/d) and mean notch diagonal lengths (d) for the pure Bi-2212 and  $Ba(C_2H_3O_2)_2$ impurity added Bi-2212 ceramic structures. Notably,  $Ba(C_2H_3O_2)_2$ impurity ion addition significantly modifies the curve profiles, indicating measurable changes in critical performance indicators, elastic recovery mechanisms, tetragonal phase stability, and resistance to deformation. The  $Ba(C_2H_3O_2)_2$  impurity directly affects the structural integrity of the Bi-2212 matrix.

The calculated  $\alpha$  and  $\beta$  parameters are summarized in Table 4. All  $\alpha$  values are positive, confirming typical ISE behavior for all samples. The  $\alpha$  parameters are found to be between 2.226 x 10<sup>-4</sup> N/ $\mu$ m and 14.845 x 10<sup>-4</sup> N/ $\mu$ m. Further, the  $\beta$  coefficients are note to be intervals of 1.484-6.740 x 10<sup>-4</sup> N/ $\mu$ m<sup>2</sup>, is attributed to the typical ISE nature.

$$H_{PSR} = 1845.4 \,\beta$$
 (8)

Load-independent Hv values in the PL regions, calculated using Eq. 7, are listed in Table 4. These values are substantially lower than experimental Hv measurements, confirming that while the PSR model is effective for analyzing load-dependent mechanical properties, it is less reliable for predicting accurate load-independent Hv values in the PL region.

## 3.5. Evaluation of mechanical performance and characteristics using MPSR model

The MPSR theoretical model refines the PSR framework by incorporating the minimum indentation load parameter (WMPSR), representing the threshold force required to initiate plastic deformation or disrupt chemical bonding in the ceramic lattice (Ref 341). This parameter provides direct insight into the elastic recovery mechanism and the onset of irreversible deformation. The MPSR model is expressed mathematically as:

$$F = W_{MPSR} + A_{0 MPSR} d + A_{1 MPSR} d^2 (9)$$

Here,  $A0_{MPSR}$  and  $A1_{MPSR}$  represent the energy losses arising from microstructural defects, plastic deformation, intergranular bonding limitations, and chemical instability. Figure 7 shows the F-d relationships for all bulk Bi2.1Sr2.0Ca1.1Cu2.0O $_{\gamma}$ +( Ba(C $_{2}$ H $_{3}$ O $_{2}$ ) $_{2}$ )x ceramic cuprates, from which  $W_{MPSR}$ ,  $A0_{MPSR}$ , and  $A1_{MPSR}$  are determined (Table 4). Positive  $W_{MPSR}$  values for all samples (ranging from 0.7228 x  $10^{-2}$  N to 8.747 x  $10^{-2}$  N) confirm the prevalence of typical ISE behavior, with elastic recovery dominating post-indentation deformation. Besides, the increment trend in the  $W_{MPSR}$  values with the Ba(C2H3O2)2 impurity ion addition stems from the systematic rise of microscopic structural problems.  $A1_{MPSR}$  parameter, closely linked to mechanical performance, decreases from 2.503 x  $10^{-4}$  N/  $\mu$ m<sup>2</sup> for the pure sample to a minimum of 1.656 x  $10^{-4}$  N/  $\mu$ m<sup>2</sup> at x = 0.13, indicating reduced resistance to deformation, degraded phase stability, and crack suppression. Besides, the decrease trend also results from the increased defect densities and reduced structural integrity. Load-independent Hv values in the PL region, computed via Eq. 9, are presented in Table 4. According to table, the results deduced from MPSR model indicate that the calculations are found to be slight lower than the load-independent Hv parameters in PL zones.

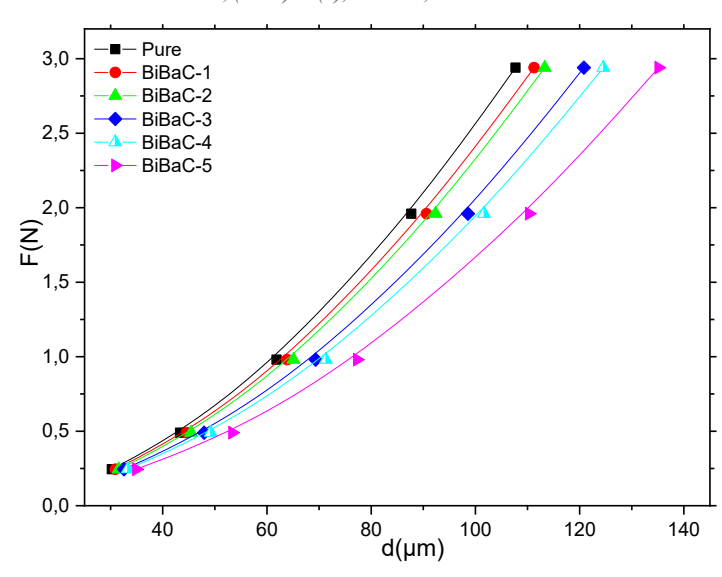


Figure 7. Alteration of the applied test load, F as a function of diagonal lengths, d under various loads for pure Bi-2212 and bulk  $Ba(C_2H_3O_2)_2$  impurity added Bi-2212 ceramic structures

To sum up, the true Hv parameter analysis within saturation limit regions for the pure and Ba(C<sub>2</sub>H<sub>3</sub>O<sub>2</sub>)<sub>2</sub> impurity added Bi-2212 ceramic structures, performed using the HK mechanical approach, yields the results summarized in Table 4. The findings reveal that the HK model provides superior accuracy compared to all other semi-empirical approaches in reproducing the experimentally measured Hv values. Among the modeling methods evaluated, the HK approach provides the most reliable and closest agreement with the actual hardness data. Consequently, it is identified as the most effective technique for assessing true hardness parameters in the plateau limit regions, while also enabling precise evaluation of mechanical performance characteristics and behavioral features of advanced ceramic materials.

### 4. Conclusion

We investigated the variations in fundamental mechanical properties and actual Vickers hardness (Hv) parameters within the PL regions of both pure Bi-2212 and Ba(C<sub>2</sub>H<sub>3</sub>O<sub>2</sub>)<sub>2</sub> impurity-incorporated Bi-2212 ceramic structures containing different concentrations of barium acetate ions. The obtained experimental results from Vickers hardness tests were evaluated semi-empirically using five recognized mechanical models, namely PSR, MPSR, ML, EPD, and HK. For clarity and precision, the discussion primarily emphasizes the EPD, MPSR, and HK models, as these provide the most consistent and reliable predictions of true Hv values in the PL regions, though the results from all models are also presented. The analysis demonstrates that increasing the Ba(C<sub>2</sub>H<sub>3</sub>O<sub>2</sub>)<sub>2</sub> impurity content gradually deteriorates the intrinsic slip systems and the crystalline integrity due to a higher density of stress concentration centers and microstructural stress raisers. This degradation at the microscopic level leads to a decline in mechanical robustness and overall structural endurance. Accordingly, the undoped Bi-2212 specimen exhibits the lowest sensitivity to applied mechanical stress, whereas the heavily doped BiBaC-5 sample presents the greatest vulnerability to external loading. Both pure and Ba(C<sub>2</sub>H<sub>3</sub>O<sub>2</sub>)<sub>2</sub>-modified Bi-2212 ceramics display a typical indentation size effect (ISE) behavior, with the pure sample showing the most pronounced ISE response. Among all the theoretical models examined, the HK approach provides hardness values in the plateau regions that best align with the experimentally determined Hv data, confirming it as the most accurate and dependable model for assessing the mechanical behavior of Bi-2212 ceramics containing various levels of Ba(C<sub>2</sub>H<sub>3</sub>O<sub>2</sub>)<sub>2</sub> impurities.

# References

Abdelhaleem, S., Alziyadi, M. O., Alruwaili, A., Alawi, M. J., Alkabsh, A., & Shalaby, M. S. (2025). BSCCO high Tc-superconductor materials: Strategies toward critical current density enhancement and future opportunities. Applied Physics A, 131(2), 151.

Askeland, D. R., Fulay, P. P., & Wright, W. J. (2010). The science and engineering of materials. Cengage Learning.

Callister, W. D., Jr., & Rethwisch, D. G. (2010). Materials science and engineering: An introduction. Wiley.

Chang, J., Yang, F., Zhang, S., Cao, H., Zhang, Y., Liu, G., Liu, J., Li, C., Li, J., & Zhang, P. (2025). Effects of La doping on the structure and superconducting properties of Bi-2212. Journal of Materials Science: Materials in Electronics, 36, 817.

Chattopadhyay, R. (2001). Surface wear: Analysis, treatment, and prevention. ASM International.

Dogruer, M., Motoki, T., Semba, M., Nakamura, S., & Shimoyama, J. (2024). Mechanical properties of Ag-added DyBa<sub>2</sub>Cu<sub>3</sub>Oy superconducting melt-textured bulks prepared by the single-direction melt growth method. Materials Today Communications, 39, 108605.

Elmustafa, A. A., & Stone, D. S. (2003). Nanoindentation and the indentation size effect: Kinetics of deformation and strain gradient plasticity. Journal of the Mechanics and Physics of Solids, 5, 357–381.

Erdem, U., Yildirim, G., Türköz, M. B., Ulgen, A. T., & Mercan, A. (2023). Change in transition balance between durable tetra gonal phase and stress-induced phase of cobalt surface-layered in Bi-2212 materials by semi-empirical mechanical models. Physica Scripta, 98(7), 075702.

Erden, M. A., Tasliyan, M. F., & Akgul, Y. (2021). Effect of TiC, TiN, and TiCN on microstructural, mechanical and tribological properties of PM steels. Science of Sintering, 53(4), 497–508.

Fallah-Arani, H., Sedghi, A., Baghshahi, S., Moakhar, R. S., Riahi-Noori, N., & Nodoushan, N. J. (2022). Bi-2223 superconductor ceramics added with cubic-shaped TiO<sub>2</sub> nanoparticles: Structural, microstructural, magnetic, and vortex pinning studies. Journal of Alloys and Compounds, 900, 163201.

Fröhlich, F., Grau, P., & Grellmann, W. (1977). Performance and analysis of recording microhardness tests. physica status solidi (a), 42, 79.

Hannachi, E., Slimani, Y., Ekicibil, A., Manikandan, A., & Azzouz, F. B. (2019). Magneto-resistivity and magnetization investigations of YBCO superconductor added by nano-wires and nano-particles of titanium oxide. Journal of Materials Science: Materials in Electronics, 30, 8805–8813.

Harabor, A., Rotaru, P., Harabor, N. A., Nozar, P., & Rotaru, A. (2023). Structural, thermal and superconducting properties of Ag<sub>2</sub>O-doped YBa<sub>2</sub>Cu<sub>3</sub>O<sub>7</sub>–x composite materials. Ceramics International, 49(9), 14904–14916.

Hassan, M. S., Mohamed, I. E., Matar, M., Abou-Aly, A. I., Awad, R., & Anas, M. (2023). Effect of hard magnetic ferrite (Ba<sub>0.5</sub>Sr<sub>0.5</sub>Fe<sub>12</sub>O<sub>19</sub>) nanoparticles on the mechanical properties of the (Bi, Pb)-2223 phase. Applied Physics A, 129(5), 333.

Hays, C., & Kendall, E. G. (1973). An analysis of Knoop microhardness. Metallography, 6, 275–282.

Jeong, S. H., Song, J. B., Choi, Y. H., Kim, S. G., Go, B. S., Park, M., & Lee, H. (2016). Effect of micro-ceramic fillers in epoxy composites on thermal and electrical stabilities of GdBCO coils. Composites Part B: Engineering, 94, 190–196.

Kara, E., Özkurt, P., & Özkurt, B. (2022). Effects of different dwell-times under low pelletization pressure on the physical properties of the Bi-2212 ceramics. Journal of Materials Science: Materials in Electronics, 33(18), 14951–14960.

Khalil, S. M. (2001). Enhancement of superconducting and mechanical properties in BSCCO with Pb additions. Journal of Physics and Chemistry of Solids, 62, 457–466.

Ling, H. C., & Yan, M. F. (1988). Microhardness measurements on dopant-modified superconducting YBa<sub>2</sub>Cu<sub>3</sub>O<sub>7</sub> ceramics. Journal of Applied Physics, 64, 1307.

Michels, B. D., & Frischat, G. H. (1982). Microhardness of chalcogenide glasses of the system Se–Ge–As. Journal of Materials Science, 17, 329–334.

Mohammed, N. H., Abou-Aly, A. I., Ibrahim, I. H., Awad, R., & Rekaby, M. (2009). Mechanical properties of (Cu<sub>0.5</sub>Tl<sub>0.5</sub>)-1223 added by nano-SnO<sub>2</sub>. Journal of Alloys and Compounds, 486, 733–737.

Müller, P., Ustinov, A. V., & Schmidt, V. V. (1997). The physics of superconductors: Introduction to fundamentals and applications. Springer.

Plakida, N. (2010). High temperature cuprate superconductors. Springer.

Saxena, A. K. (2012). High-temperature superconductors (Vol. 125). Springer Science & Business Media.

Sheahen, T. P. (2002). Introduction to high-temperature superconductivity (1st ed.). Kluwer Academic Publishers.

Slimani, Y., Almessiere, M. A., Hannachi, E., Baykal, A., Manikandan, A., Mumtaz, M., & Azzouz, F. B. (2019). Influence of WO<sub>3</sub> nanowires on structural, morphological and flux pinning ability of YBa<sub>2</sub>Cu<sub>3</sub>Oy superconductor. Ceramics International, 45(2), 2621–2628.

Smith, W. F. (2001). Principles of materials science and engineering. McGraw-Hill.

Takayama-Muromachi, E. (1998). High-pressure synthesis of homologous series of high critical temperature (Tc) superconductors. Chemistry of Materials, 10(10), 2686–2698.

Tancret, F., Monot, I., & Osterstock, F. (2001). Toughness and thermal shock resistance of YBa<sub>2</sub>Cu<sub>3</sub>O<sub>7</sub>–x composite superconductors containing Y<sub>2</sub>BaCuO<sub>5</sub> or Ag particles. Materials Science and Engineering: A, 298, 268–283.

Tarkanian, M. L., Neumann, J. P., & Raymond, L. (1973). The science of hardness testing and its research application. American Society for Metals.

Turkoz, M. B., Zalaoglu, Y., Turgay, T., Ozturk, O., & Yildirim, G. (2019). Effect of homovalent Bi/Ga substitution on propagations of flaws, dislocations and crack in Bi-2212 superconducting ceramics: Evaluation of new operable slip systems with substitution. Ceramics International, 45, 22912–22919.

Ulgen, A. T., Yildirim, G., & Erdem, U. (2025a). Alteration of electrical features of Bi-2212 crystal structure with barium acetate. In Proceedings of the II. International Future Engineering Conference (IFEC 2025) (pp. 480–488).

Ulgen, A. T., Yildirim, G., & Erdem, U. (2025b). Role of barium acetate impurity on superconducting transition properties of Bi-2212 cuprates. In Proceedings of the II. International Future Engineering Conference (IFEC 2025) (pp. 489–498).

Xu, A., Jiang, J., Tarantini, C., Kametani, F., Hellstrom, E., & Larbalestier, D. C. (2024). Flux pinning enhancement of Bi-2212 tapes by increasing Sr content. IEEE Transactions on Applied Superconductivity, 34(3), 1–5.

Zagura, P., Kim, I., Follows, F., Barker, C., Melhem, Z., Twin, A., Ball, S., Grovenor, C., Speller, S., & Mousavi, T. (2024). Development of persistent joints for superconducting Bi-2212 coils. Superconductor Science and Technology, 37, 055003.

Zalaoglu, Y., Akkurt, B., Oz, M., & Yildirim, G. (2017). Transgranular region preference of crack propagation along Bi-2212 crystal structure due to Au nanoparticle diffusion and modeling of new systems. Journal of Materials Science: Materials in Electronics, 28, 12839–12850.

Zalaoglu, Y., Turgay, T., Ulgen, A. T., Erdem, U., Turkoz, M. B., & Yildirim, G. (2020). A novel research on the subject of the load-independent microhardness performances of Sr/Ti partial displacement in Bi-2212 ceramics. Journal of Materials Science: Materials in Electronics, 31(24), 22239–22251.

Zhao, X., Tian, H., Qi, Y., Lu, X., Ma, Y., Li, H., ... & Wang, T. (2024). A novel method to enhance the superconducting properties of Bi<sub>2</sub>Sr<sub>2</sub>CaCu<sub>2</sub>O<sub>8</sub>+δ superconducting thin films by self-assembly NiO nanorods. Ceramics International, 50(19), 35388–35396.